Reports

Experiments on Salt Fingers in a Hele Shaw Cell

J. TAYLOR AND G. VERONIS

"Salt fingers" are generated when a slowly diffusing solute overlies a more rapidly diffusing solute in a gravitationally stable fluid. The phenomenon is important in many areas of science; for example, it affects the temperature and salinity structure in the upper half of the ocean, the production of crystals when liquid alloys solidify, and the distribution of properties in magma chambers below the earth's crust. The evolution of a salt finger from initial instability to a fully developed feature is difficult to follow in a fluid because of the close-packed array of cells that is formed. However, when the fluid is contained in a Hele Shaw cell, individual fingers occupy the entire gap width, thereby enabling the experimenter to monitor and record the evolution much more easily. The instability of an array of wide fingers to disturbances that lead to (preferred) smaller scales is documented in a sequence of photographs, and a qualitative, physically consistent argument is offered to explain the instability.

A GRAVITATIONALLY STABLE, TWO-layer fluid system with a less diffusible solute (*S*) above and a more diffusible solute (*T*) below can become unstable to perturbations that evolve into a close-packed array of alternately rising and sinking columns of fluid from one reservoir to the other. Because the original experiment (*1*) and a subsequent analysis (*2*) were carried out with a system that used salt as the solute and heat to generate a stabilizing gradient, the generated columns are called "salt fingers."

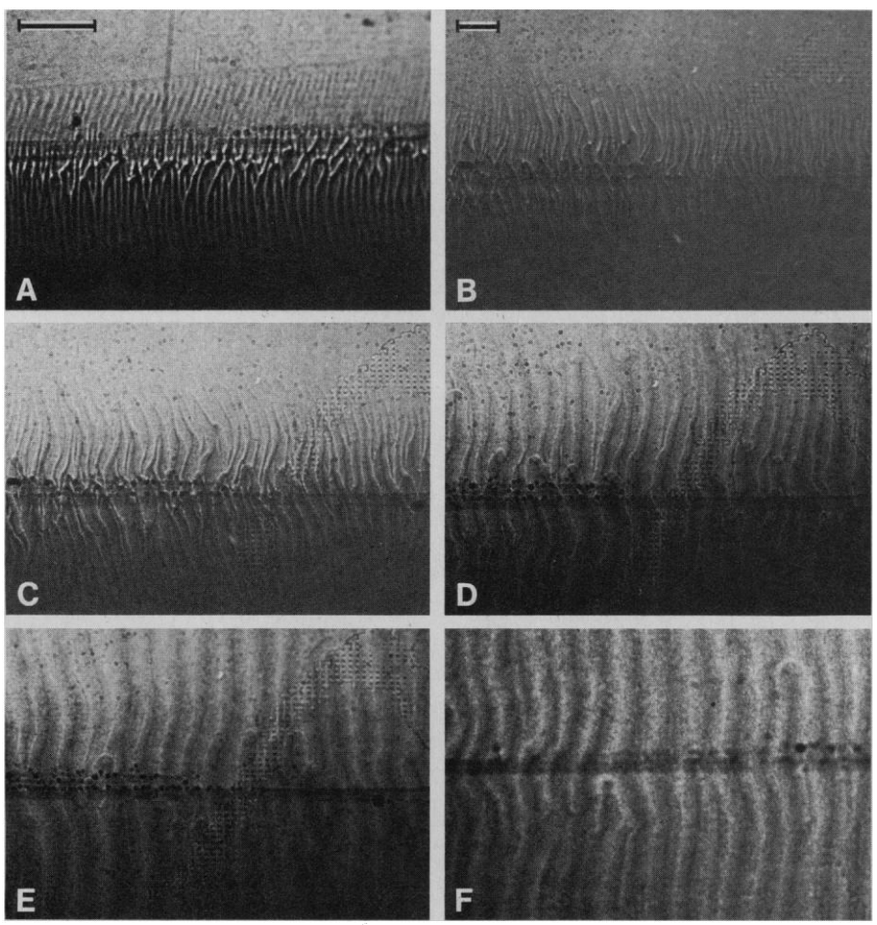

Fig. 1. Shadowgraphs of the growth of salt fingers from an initially sharp interface in a Hele Shaw cell. The pictures were taken at (A) 0.8, (B) 2.4, (C) 4.6, (D) 14.6, (E) 40.9, and (F) 146.6 hours after the initiation of the experiment. The mesh pattern (B to E) is a pattern etched into the glass surface of the cell, and the small circles are air bubbles. Scale bar, 1 cm (B to F have the same scale).

Although there is an extensive literature on salt fingers (*3–6*), little is known about the evolution of fingers from the initial instability to fully developed columns. We now describe observations from experiments with sugar and salt in a Hele Shaw cell made up of two glass plates (1 by 30 by 50 cm each) separated by a 0.1-cm spacer. The purpose of the experiments was to observe the structure of individual salt fingers as they evolve and thus to describe the phenomenology that must eventually be explained by a pertinent theory. The Hele Shaw configuration is particularly appropriate for such a purpose because after a short period the preferred horizontal scale of the motion is larger than the gap width, and an individual cell can easily be visualized.

Either directly (*7*) or by analogy with a regular fluid system, it can be shown that the horizontal scale, l, of the finger with maximum growth rate in a Hele Shaw cell is the buoyancy layer scale, $(\mu\kappa_T/g\alpha T_z)^{1/2}$, where κ_T is the diffusivity of T, g is the gravitational acceleration, and αT_z is the contribution of T to the horizontally averaged vertical density gradient. The parameter μ equals $12\nu/d^2$ (where d is the gap width and ν is the kinematic viscosity) and corresponds to the D'Arcy dissipation coefficient in a porous medium (*7*). When the plates of the Hele Shaw cell are inclined toward the horizontal, the effect of gravity is confined to the component parallel to the plates. This makes it possible to alter the preferred scale of motion at will. In particular, once a cellular pattern is established, changing the angle of inclination changes the preferred cell size, and the adjustment from one cell size to another can be studied. It is important to understand such an adjustment because similar effects must arise in a regular fluid when the properties of the upper and lower reservoirs change on a short time scale.

We first describe the sequence of events with the long side of the tank inclined 10° to the horizontal. A barrier (height, 0.3 cm) separating the lower salt solution (density, 1.0186 g cm^{-3}) from the upper sugar solution (density, 1.0090 g cm^{-3}) was slowly withdrawn at $t = 0$ (t, time). Almost immediately, an array of narrow fingers formed at the interface. Because of the initially large

J. Taylor, Research School of Earth Sciences, Australian National University, Canberra ACT 2601, Australia.
G. Veronis, Department of Geology and Geophysics, Yale University, New Haven, CT 06511.

gradient, T_z, the scale of the fingers was very small (visually estimated at 0.03 cm), and more than one finger occupied the gap width. These fingers redistribute the salt and reduce T_z rapidly, so that within minutes the scale of the fingers increased to about 0.1 cm. Figure 1A shows the residual three-dimensional structure at the interface and a uniform upper boundary of penetration of the finger pattern with about eight cells per centimeter. (The flow was observed by shadowgraph; that is, a beam of parallel light through the experiment is refracted by the different solute concentrations, and the image is recorded at the focal point of the refracted beam. In Fig. 1A the camera was closer to the image than it was for subsequent photographs, as indicated by the larger scale bar.)

As the fingers evolve, T_z continues to decrease, and the preferred scale increases. Wider cells penetrate from the upper and lower extremes of the finger region, where T_z is smaller. Figure 1B depicts the structure at t = 2.4 hours with a larger scale (0.3 cm) above and below and a smaller scale structure, in which the cells meet near the interface. At t = 4.6 hours (Fig. 1C), a more evolved, large-scale pattern is evident, although residual small-scale structure is still present. By t = 14.6 hours (Fig. 1D), features with a scale of 0.6 cm dominate the convection pattern. Fingers that have partially penetrated give rise to apparent branching of cells that they meet. In Fig. 1E (t = 40.9 hours), 0.8-cm features occupy nearly the entire tank. Fingerlike and bulbous tips are evidence of the continued penetration of new fingers from the outer edges of the convective region. The final photo (Fig. 1F), at t = 146.6 hours, exhibits a slightly larger finger scale and partial penetration of some fingers.

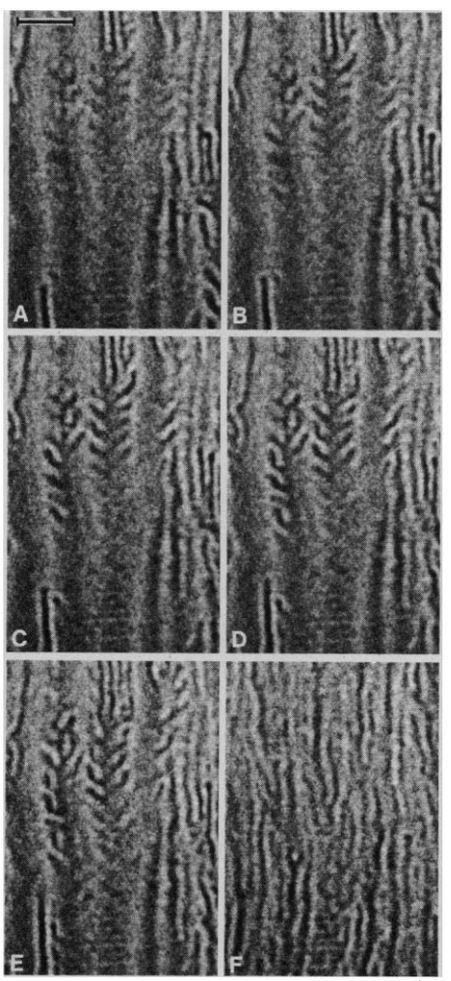

Fig. 2. Shadowgraphs of the instability of wide salt fingers in a Hele Shaw cell subjected to a sudden change in effective gravity. The pictures were taken (A) 13, (B) 14, (C) 15, (D) 16, (E) 17, and (F) 22 minutes after the tank was returned to the vertical. Scale bar, 1 cm.

The overall picture is, therefore, one of continuous evolution. As the salt fingers grow taller they decrease the stabilizing gradient T_z, and this in turn increases the preferred scale of the cells. The system does not reach a steady state (although the principal dynamical balance may possibly be obtained from a steady model with the appropriate values for parameters such as T_z). There was no evidence in this experiment of a transition to random, large-scale convection at the boundaries of the finger region. However, in experiments with larger concentrations of salt and sugar, but still with the same gravitational stability, large convection cells were generated in the reservoirs above and below the fingers.

The Hele Shaw configuration makes it possible to study the manner in which fingers of the preferred scale can develop from a field of either larger or smaller scales. For example, in the experiment described above the final pattern of fingers had a scale of about 0.8 cm. The tank was then raised to an upright position, so that the effective gravity is g. The preferred cell size is thereby reduced to $[\sin(10°)]^{1/2}(0.8\text{ cm}) = 0.3$ cm. How does the fluid adjust to the smaller scale?

The series of photographs in Fig. 2 shows that the large-scale fingers become unstable to a smaller scale disturbance inclined about 45° from the axis of the cell. The resulting fernlike pattern extends downward from the middle of high S cells to the middle of low S cells on either side. At the ends of these inclined cells the T anomaly has diffused out, and the fingers turn toward the vertical and join with similar features above and below to form long narrow cells. The last photograph (Fig. 2F) shows an advanced stage of development with no trace of the fern pattern. At a much later stage, straight, narrow cells extend from the top to the bottom of the tank.

A physical explanation of the instability is given in terms of the heat (T)-salt (S) system. Figure 3A shows the equilibrium T structure of a wide cell. High T is convected downward in the left finger and low T upward in the right finger. Horizontal diffusion generates the sinusoidal pattern shown. When the tank is placed upright, the buoyancy boundary layer (the effective diffusion scale) is smaller, and the high T value in the left finger is smoothed only in the thinner boundary layer, leaving a plateau in the middle. The fluid in the middle of the cell is warmer and saltier than in the boundary layer. A sinusoidal-like perturbation near the outer edge of the boundary layer (dashed curve in Fig. 3C) allows warmer fluid from the middle region to penetrate into the boundary layers where it is cooled by thermal diffusion, retains its salt, and thereby

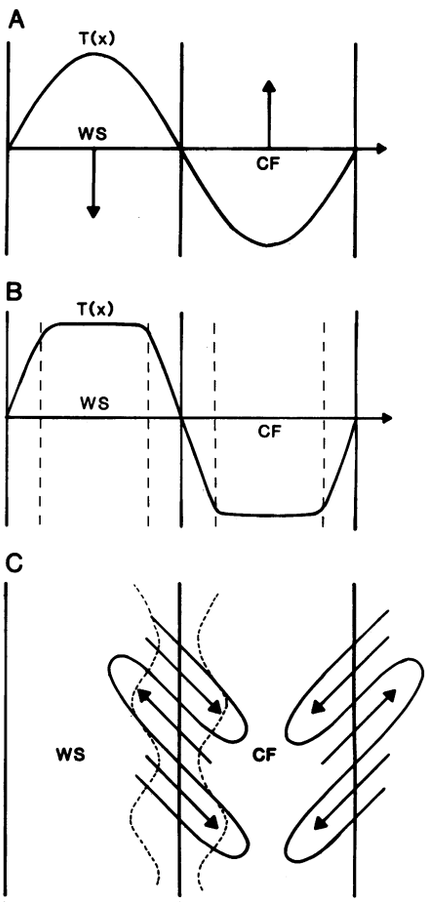

Fig. 3. (A) A sketch of the horizontal temperature profile through upgoing, cold fresh (CF) and downgoing, warm salty (WS) equilibrium wide fingers. The arrows indicate the direction of fluid motion. (B) The temperature profile soon after the effective gravity has been increased by returning the tank to the vertical. (C) A sketch of the motions arising from the instability of the salt fingers.

becomes cool and salty. Similarly, fluid from the boundary layer penetrates toward the middle and is warmed so that it becomes warm and fresh. A similar argument is valid in the rising cell on the right. The net effect is to generate a slanted motion, as shown, with warm fresh fluid rising toward the left and cold salty fluid sinking toward the right to form one-half of the fernlike pattern (the other half is drawn in by symmetry).

When the narrow finger pattern of the upright Hele Shaw cell has been established, the tank may be inclined toward the horizontal so that the preferred finger scale is larger. In this case there is no rapidly growing instability. Wider cells were observed to form near the top and bottom of the salt finger region and to penetrate toward the middle. This process for the formation of wider cells is the same as that observed during the rundown of the system in the first experiment described above.

REFERENCES AND NOTES

1. H. Stommel, A. B. Arons, D. Blanchard, *Deep Sea Res.* **3**, 152 (1956).
2. M. E. Stern, *Tellus* **12**, 172 (1960).
3. J. S. Turner, *Buoyancy Effects in Fluids* (Cambridge Univ. Press, Cambridge, 1973).
4. H. E. Huppert and J. S. Turner, *J. Fluid Mech.* **106**, 299 (1981).
5. C. F. Chen and D. H. Johnson, *ibid.* **138**, 405 (1984).
6. J. S. Turner, *Annu. Rev. Fluid Mech.* **17**, 11 (1985).
7. J. W. Taunton, E. N. Lightfoot, T. Greene, *Phys. Fluids* **15**, 748 (1972).

8. Supported in part by NSF grant OCE-8410154.

15 July 1985; accepted 16 October 1985

The Accumulation of Cosmogenic Chlorine-36 in Rocks: a Method for Surface Exposure Dating

FRED M. PHILLIPS, BRIAN D. LEAVY*, NANCY O. JANNIK, DAVID ELMORE, PETER W. KUBIK

Because of the reaction of cosmic rays with elements in minerals, chlorine-36 accumulates in rocks exposed at the earth's surface. This suggests that the ratio of chlorine-36 to stable chloride can be used as a geochronometer. Reasonable agreement has been obtained between measurements of chlorine-36 in volcanic rocks of known age and calculations of chlorine-36 production based on rock composition and cosmic-ray flux. The buildup of chlorine-36 should be a useful means for measuring the surface exposure time of young volcanic rocks and geomorphic features in the age range of 10^3 to 10^6 years.

COMMONLY USED RADIOMETRIC techniques for the dating of rocks are of two types. The first, exemplified by the K-Ar, Rb-Sr, and U-Th methods, makes use of the buildup of daughter products from primordial radionuclides. The second approach uses the decay of cosmogenic isotopes that are produced in the atmosphere and then incorporated into terrestrial reservoirs. Examples of this approach include standard ^{14}C and ^{10}Be dating. We now describe a third approach: measurement of the buildup of cosmogenic radionuclides in geological materials exposed to cosmic rays at the earth's surface. Whereas the first two techniques measure the time since the object to be dated became a geochemically closed system, the third technique measures the time of the object's exposure on the surface of the earth. Therefore, this method should allow chronologies to be established for presently undatable geomorphic features as well as for certain materials that can be dated only with difficulty by means of the first two techniques (for example, low-potassium volcanic rocks less than 500,000 years old).

Radionuclides useful for cosmogenic buildup dating should have half-lives ($t_{1/2}$) long enough to be applied on geological time scales but short enough that there will be no primordial material present. Possible candidates include ^{36}Cl ($t_{1/2}$, 3×10^5 years), ^{26}Al ($t_{1/2}$, 7.2×10^5 years), and ^{10}Be ($t_{1/2}$, 1.6×10^6 years). We have investigated the accumulation of ^{36}Cl in rocks for cosmogenic buildup dating. The use of ^{36}Cl for this purpose was first suggested 30 years ago (*1*) but was not successful at that time because of insufficient analytical sensitivity; tandem accelerator mass spectrometry (TAMS) (*2*) has now overcome this limitation.

Chlorine-36 has several useful characteristics for buildup dating: (i) it builds up to measurable levels relatively quickly because the product element (chlorine) generally is present only in trace quantities; (ii) ^{36}Cl activities produced by nuclear processes within the rock (due to uranium and thorium) are low enough that they should be much less than the cosmogenic activity after 5000 years of exposure or less; and (iii) the mobile and hydrophilic nature of chlorine should aid in the separation of the ^{36}Cl produced within the rock from meteoric (atmospheric) ^{36}Cl. Recent research (*3*) has indicated that even relatively immobile radionuclides such as ^{137}Cs can penetrate rocks in a short time. Chlorine-36 is more hydrophilic than ^{10}Be or ^{26}Al, and this feature may be useful in cases where the separation of meteoric and in situ components is necessary.

Chlorine-36 is produced within rocks by several reactions. In many rocks the primary reaction is thermal neutron activation of ^{35}Cl. The production rate, ψ_n (in atoms of ^{36}Cl per kilogram per year), is given by

$$\psi_n = \phi_n \frac{\sigma_{35} N_{35}}{\sum_i \sigma_i N_i} \quad (1)$$

where ϕ_n is the thermal neutron flux at sea level [about 10^6 n kg^{-1} year^{-1}, although the exact value is uncertain (*4*)], σ_{35} is the thermal neutron capture activation cross section of ^{35}Cl (43 barns), N_{35} is the concentration of ^{35}Cl (in atoms per kilogram), σ_i is the thermal neutron absorption cross section for each element i, and N_i is the concentration of each element.

A second mechanism of production, which is more important in rocks with low amounts of chlorine, is direct spallation of potassium and calcium. Yokoyama and coworkers (*5*) have calculated sea-level production rates of 2670 atoms of ^{36}Cl per kilogram per year per percent K_2O for potassium (ψ_K) and 710 atoms of ^{36}Cl per kilogram per year per percent CaO for calcium (ψ_{Ca}). Spallation production from titanium and iron is probably insignificant at the earth's surface because of attenuation of the highly energetic cosmic rays by the atmosphere. Negative muon capture by ^{40}Ca is a minor reaction that produces ^{36}Cl (*6*). This reaction becomes significant at

Fred M. Phillips, Brian D. Leavy*, and Nancy O. Jannik, Geoscience Department and Geophysical Research Center, New Mexico Institute of Mining and Technology, Socorro 87801.
David Elmore and Peter W. Kubik, Nuclear Structure Research Laboratory, University of Rochester, Rochester, NY 14627.

* Present address: Los Alamos National Laboratory, Los Alamos, NM 87545.